National Physical Laboratory

Report

NPL REPORT IR 4

Literature review and simulations for total absorption calorimetry in a proton beam

Hugo Palmans, David Shipley, Jozef Martinkovič and Jozef Dobrovodský

NOT RESTRICTED

DECEMBER 2007

National Physical Laboratory | Hampton Road | Teddington | Middlesex | United Kingdom | TW11 0LW
Switchboard 020 8977 3222 | **NPL Helpline** 020 8943 6880 | **Fax** 020 8614 0446 | **www.npl.co.uk**

Department for Innovation, Universities & Skills

LITERATURE REVIEW AND SIMULATIONS FOR TOTAL ABSORPTION CALORIMETRY IN A PROTON BEAM

Hugo Palmans[1], David Shipley[1], Jozef Martinkovič[2] and Jozef Dobrovodský[2]

[1]Radiation Dosimetry Team, National Physical Laboratory
[2]Slovak Institute of Metrology, Bratislava, Slovakia

ABSTRACT

A new 72 MeV cyclotron is being built in Bratislava, Slovakia, which will have a dosimetry beam line with a possible extension for time-of-flight measurements. The combination of time of flight measurements with total absorption calorimetry offers an interesting potential route of providing an off-site beam energy calibration service. This report provides some literature review as well as Monte Carlo and heat transfer simulations to support a total absorption calorimeter design that could be established through collaboration between NPL and SMU.

ISSN 1754-2952

National Physical Laboratory
Hampton Road, Teddington, Middlesex, TW11 0LW

Approved on behalf of the Managing Director, NPL
by *Dr Martyn Sene*, Director, *Division Quality of Life*

CONTENTS

1. INTRODUCTION

A new 72 MeV cyclotron is being built in Bratislava, Slovakia on the site of the Slovak Institute of Metrology (SMU). Among the six planned beam lines (some of them which will be split further) one will be devoted to radiotherapy of eye tumours and another one to dosimetry. The dosimetry beam line will possibly be extended with a hall sufficiently large for time-of-flight measurements. The combination of time of flight measurements with total absorption calorimetry offers an interesting route of providing a service of off-site characterisation of proton beam energy and energy distributions. Other highly valuable applications would be the determination of the range-energy relation, stopping cross sections and non-elastic nuclear cross sections of incident protons.

This report provides a literature review on total absorption calorimetry and useful calorimetry designs as well as Monte Carlo and heat transfer simulations to support a total absorption calorimeter design that could be established through collaboration between SMU and NPL.

2. LITERATURE REVIEW

Applications of calorimeters to radiotherapeutic dosimetry can be divided into total absorption calorimetry and calorimetry to obtain absorbed dose in a point. The latter method constitutes of measuring the radiation induced temperature rise ΔT_{med} in a point (or a small isolated volume) in a medium and deriving absorbed dose to the medium D_{med} as $D_{\mathrm{med}} = c_{\mathrm{med}} \cdot \Delta T_{\mathrm{med}}$, where c_{med} is the specific heat capacity of the medium, usually obtained from an electrical calibration. This method is widely used to measure absorbed dose to water in primary standards (Allisy-Roberts et al. 2005). In total absorption calorimetry incident particles are completely absorbed in the calorimeter and the total energy E_{p} of the particle is related to the temperature rise as $E_{\mathrm{p}} = C_{\mathrm{med}} \cdot \Delta T_{\mathrm{med}}$, where C_{med} is the heat capacity of the medium. Total absorption calorimeters operated at cryogenic temperatures are used in elementary particle physics as spectrometers (Twerenbold 1996). Also in radioactivity measurements total absorption bolometers (4π-calorimeters) operated at cryogenic temperatures are used as spectrometers (Leblanc et al. 2006) or for total activity measurements (Leblanc et al. 2002 and Stump et al. 2005). In all these applications it is assumed that the deposited energy is entirely converted into heat and thus, that no exothermic or endothermic change of state takes place.

Some experiments have been performed specifically to measure the chemical heat defect by measuring the temperature rise in a total absorption calorimeter receiving a known amount of ionising radiation energy. Assuming that the chemical heat defect for aluminium is zero, Fleming and Glass (1969), McDonald and Goodman (1982) and Schulz et al. (1990) used a technique with a double absorber consisting of aluminium and A-150 forming a single heat capacity to determine the chemical heat defect of A-150. They consistently found an endothermic heat defect and derived a correction factor of 1.040 ± 0.015 for an A-150 calorimeter. Schulz et al. (1990) have measured the chemical heat defect for graphite using the same technique, confirming within the experimental uncertainty the idea that the chemical heat defect in graphite is zero. Since the latter paper provides a calorimeter design with a rotatable core in vacuum that could be very valuable for the design of a total absorption calorimeter, a schematic drawing is given in figure 1. For more details we refer to the paper of Schulz et al. (1990).

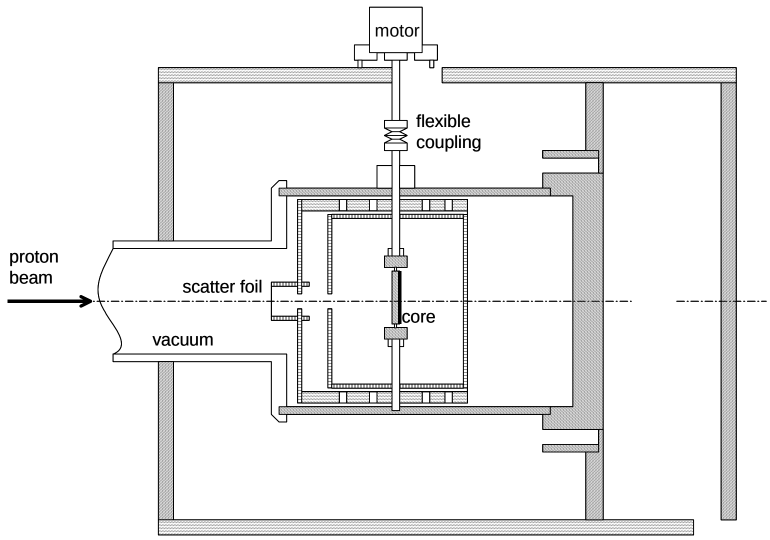

Figure 1. Total absorption calorimeter for low-energy protons with a rotatable composite Al-A150 or Al-graphite absorber used by Schulz et al. (1990) to measure the heat defect of A150 and graphite. [Adapted from Schulz et al. (1990)]

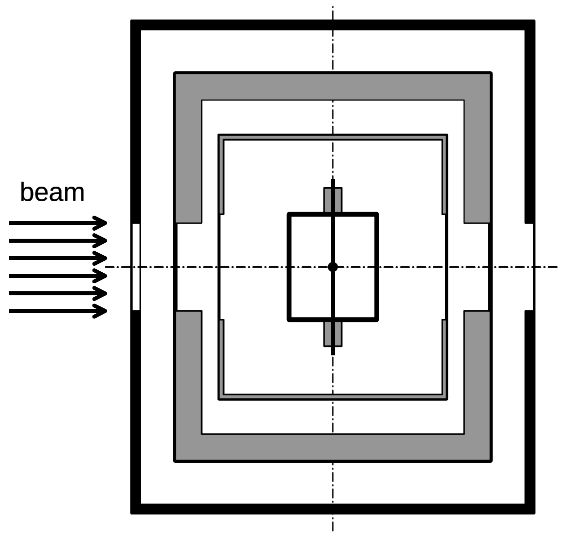

Figure 2. Water calorimeter used by Brede et al (2006) to measure absorbed dose to water in proton beams (as well as in other beams). [Adapted from Brede et al (2006)]

Brede et al. (1997) designed an experiment to determine the chemical heat defect of water for proton beams in an absolute way. The principle is very similar as the one used to determine the heat defect of A-150 using a combined aluminium/water absorber. A 19 MeV proton beam was completely absorbed either in the water part or in the aluminium part. Preliminary results showed a chemical heat defect that was smaller than 1%. Earlier, Selbach et al. (1992) also performed such experiment but using soft x-rays which were (almost) totally absorbed in either the water or steel section of the absorber. In the case of soft x-rays, incomplete absorption and scatter of the beam are more difficult to determine than for protons.

Brede et al. (2000, 2006) developed a water calorimeter for absolute calorimetry that was strongly based on the design of the total absorption calorimeters. Since the absorbing core is positioned in a vacuum this design would be very suitable to be implemented at the end of the time of flight tube. A schematic diagram of the calorimeter is given in figure 2. For more details we refer to Brede et al (2006).

3. SIMULATIONS

3.1. Monte Carlo simulations

Monte Carlo simulations were performed using the codes MCNPX, Geant4 and McPTRAN.MEDIA. They are described below before a description of the simulated problem is given.

3.1.1. MCNPX (Monte Carlo N-Particle Transport Code System for Multiparticle and High Energy Applications)

MCNPX (Waters, 2002) is a general purpose Monte Carlo radiation transport code that tracks all elementary particles up to GeV range energies. Version MCNPX 2.4.0 combines the older codes MCNP4C3, MCNPX 2.3.0, LAHET 2.8 and CEM. The most important feature for this work are a condensed history scheme for electromagnetic proton interactions, the inclusion of non-elastic nuclear interactions and transport of secondary particle cascades from nuclear interactions. Three-dimensional geometries built of first- and second-degree surfaces and some special fourth-degree surfaces can be treated. For the lower energy region of neutrons and photons point wise continuous-energy cross section data are used. It contains intermediate interaction physics including intranuclear cascade models, multistage pre-equilibrium models, the Fermi-breakup model, the evaporation model and nuclear level densities. Various variance reduction techniques are implemented as well as scoring tallies and data analysis tools. The simulated particle range (for the isotopes relevant for this work) is restricted to neutrons in the LA150 library from 0.0 - 150.0 MeV in tabular range, neutrons from 1.0 MeV in physics model regime, protons from 1.0 to 150.0 MeV in tabular range, protons from 1.0 MeV in physics model regime, photons from 1 keV - 100 GeV and photonuclear interactions from 1.0 to 150.0 MeV in tabular range. The simulations were performed with two models for proton nonelastic nuclear interaction and production cross sections: the default and the lib-24h library. An additional minor difference between the two simulations was that in the default calculation the natural composition of carbon (1.1% ^{13}C and 98.89% ^{12}C) was used whereas in the calculation with the lib-24 data 100% ^{12}C was assumed.

3.1.2. Geant4

Geant4 (Agostinelli et al. 2003) is a toolkit for the simulation of particle transport through matter. Geant4 is written in C++ and provides a complete set of tools for all the domains of detector simulation. It comes with an abundant set of physics processes to handle the diverse interactions of particles with matter across a wide energy range, as required by Geant4 multi-disciplinary nature and for many physics processes a choice of different models is available. Specifically for proton beams in the clinical energy range, there is some sensitivity to the nuclear interaction model used in the simulation. It is generally recommended to use the low-energy models but it is not obvious from the literature if this is the best choice for applications in the proton therapy range. Paganetti and Gottschalk (2003), for example, recommend the use of the pre-compound nuclear interaction model for energies below 150 MeV and the low-energy model for higher energies.

In this work, simulations were performed using Geant4 version 8.3 for three different nuclear interaction models: the Bertini (QGSP_BERT), Binary Intranuclear Cascade (QGSP_BIC) and pre-compound (PRECO) models. Neutrons produced from non-elastic nuclear interactions were transported using the standard (default) models for elastic and inelastic scattering, capture and fission with point-wise cross section data taken from the ENDF/B-VI evaluated nuclear data library. For electromagnetic interactions, the low-energy models were used for electrons and photons and also for protons (and other ions) using the default ICRU49 stopping power parameterisation. The production cut-offs for photons, electrons and positrons were set to a range of 1 mm (it was verified for one set of simulations that lowering it to 0.1 mm made no significant difference). No variance reduction techniques were used.

3.1.3. McPTRAN.MEDIA

This code is derived from PTRAN (Berger, 1993), which uses the Monte Carlo method to simulate the transport of proton beams in water for protons with energies under 255 MeV. Multiple scattering and Coulomb interaction energy loss mechanisms are taken into account along with nonelastic nuclear interactions. PTRAN calculates deposition of energy as a function of depth and radial distance from the beam, energy spectra of the primary protons as function of depth. The code uses a condensed-random-walk Monte Carlo scheme (Berger, 1963), and takes into account energy-loss straggling in Coulomb collisions with atomic electrons, multiple-scattering deflections due to elastic scattering by atoms and energy loss in nonelastic nuclear reactions. Secondary particles are not tracked.

Since only water can be simulated, Palmans and Verhaegen (1997) developed a code that could handle other media, which was further developed as McPTRAN.MEDIA and described in detail by Palmans (2005). This implementation required modifications to the material data generation programs, the scoring algorithms and the transport algorithm, especially with respect to the crossing of boundaries.

3.1.4. Simulated geometry

A simple cylindrical graphite, aluminium or copper absorber, as shown in figure X, was modelled in all the Monte Carlo simulations. The dimensions were chosen such that the primary beam is completely absorbed, i.e. the length and the radius were larger than 1.05 times the continuous slowing down range in each materials. This results in lengths and radii of 3.0 cm for graphite, 2.2 cm for aluminium and 0.8 cm for copper. In the simulations with McPTRAN.MEDIA, transport of secondary particles is not modelled but the energy loss in non-elastic nuclear interactions is calculated in-line as well as the fraction of this energy that is transferred to kinetic energy of charged particles. This fraction was assumed to be deposited locally and thus contributes to the energy deposition in the absorber. The remainder of the energy loss in non-elastic nuclear interactions goes to neutrons and gamma-photons or is converted into rest mass. In McPTRAN.MEDIA, the energy transferred to neutrons and gamma-photons is assumed to escape the absorber and thus the small contribution which is deposited in the absorber is not included. MCNPX and Geant4, on the other hand, do include this contribution. MCNPX simulations with five times larger absorber dimensions were performed to evaluate this neutron and gamma contribution as a function of absorber size.

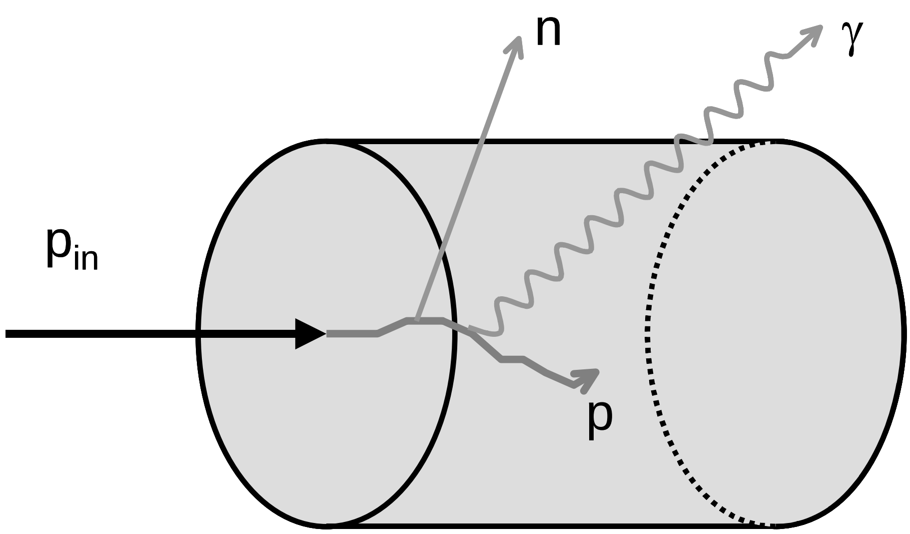

Figure 3. Simple cylindrical geometry used for the Monte Carlo simulations. The dimensions were chosen such that the primary protons are completely absorbed.

3.2. Conductive heat transfer simulations

Heat transfer within the absorber during and after the irradiation was simulated using a home written program using the finite differences method. It was previously used in heat transfer simulations for water calorimetry (Palmans 1999) and modified here to simulate the geometry in figure 4.

Table 1. Material properties for the heat conduction simulations.

Material	ρ (kg m^{-3})	c (J kg^{-1} K^{-1})	k (W m^{-1} K^{-1})
Graphite	1767	726	134
Aluminium	2700	894	237
Copper	8900	383	400

The medium was homogeneous graphite, aluminium or copper. The mass density, specific heat capacity and thermal conductivity were taken from Palmans et al. (2004) for graphite and from Kaye and Laby (1995) for aluminium and copper and are listed in table 1. The size of the phantoms was 10 cm length and 10 cm diameter in most simulations but some simulations were performed with smaller phantom dimensions (1 cm diameter and lengths of 3 cm, 2.3 cm and 0.85 cm for graphite, aluminium and copper, respectively). A simplified model of the dose distribution by the pulses in the phantom was assumed as is shown in figure 4; the volume receiving dose is cylindrical with a uniform lateral dose distribution and a Monte Carlo calculated depth dose distribution for a 72 MeV mono-energetic beam using McPTRAN.MEDIA. Since this is a qualitative assessment of the heat transfer, not much concern is given to how good this calculated depth dose distribution is.

The diameter of the volume that receives a dose was either 2 mm or 20 mm and the pulses with a duration of 1 ns came in trains of 10 or 100 with a frequency of either 1 MHz or 20 kHz. The dose per pulse was based on a current of 1 μA at 1 MHz resulting in about 3 cGy per pulse at the phantom surface. These beam characteristics are anticipated to be achievable at the new 72 MeV cyclotron facility.

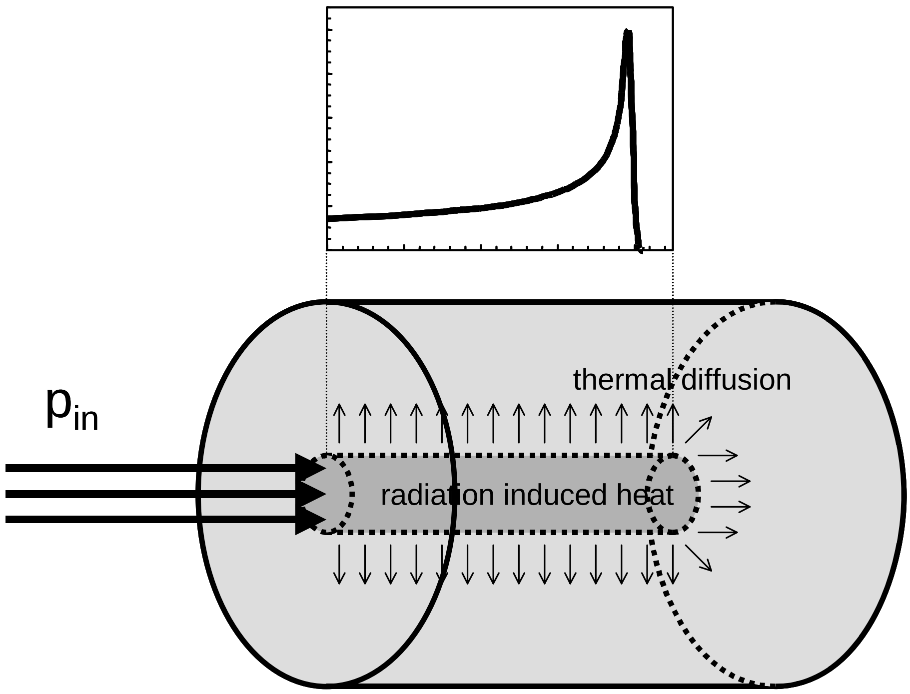

Figure 4. Geometry of heat transfer simulations.

4. RESULTS

4.1. Monte Carlo calculations

Table 2 shows the Monte Carlo simulated results of the lost energy fraction. It is clear that the three Monte Carlo codes and the different data sets are in reasonable agreement but there is nevertheless considerable variability and there are some more substantial deviations (the graphite value obtained with the default MCNPX result and the copper result obtained with McPTRAN.MEDIA). These are purely due to the difference in data-sets which are used.

One option is to use the mean values over all the models. This would lead to a value of 2.1% for graphite and 2.3% for aluminium and copper with standard deviations of 0.2% for graphite and aluminium and 0.3% for copper. These standard deviations would be acceptable as a contribution to the uncertainty.

Table 3 presents the MCNPX results of the lost energy fraction for different absorber sizes and shows that for the larger phantom sizes a small additional component of 0.1% to 0.2% of energy from neutrons and or photons is deposited.

Table 2. Monte Carlo calculated fractions in percent of the energy that is lost by the primary proton in the absorber but not converted into heat calculated with the three Monte Carlo codes and various models or data sets for nonelastic nuclear interactions.

Absorber material	MCNPX		PTRAN	GEANT4		
	default	lib-24h		QGSP_BERT	QGSP_BIC	PRECO
Graphite	1.7%	2.2%	2.1%	2.0%	2.3%	2.3%
Aluminium	2.5%	2.0%	2.1%	2.4%	2.5%	2.3%
Copper	2.4%	2.3%	2.9%	2.2%	2.3%	1.9%

Table 3. Monte Carlo calculated fractions in percent of the energy that is lost by the primary proton in the absorber but not converted into heat for different phantom sizes calculated with MCNPX (R and L have equal values of 3.0 cm, 2.2 cm and 0.8 cm for graphite, aluminium and copper, respectively).

Absorber size		Graphite	Aluminium	Copper
R	L	1.74%	2.47%	2.44%
R	5 × L	1.72%	2.43%	2.40%
5 × R	L	1.73%	2.43%	2.41%
5 × R	5 × L	1.66%	2.30%	2.25%

4.2. Heat transfer simulations

Figure 5 shows the temperature drifts as a function of time in graphite during and after irradiation with the trains of proton pulses. The drift curves during and after irradiation are shown on different scales for visualisation purposes.

Figures 5a-d show that when 10 or 100 pulses with a frequency of 1 MHz are delivered the temperature increase due to the irradiation is not deformed (i.e. proportional to the number of pulses) and the entire pulse train can be regarded as a single pulse for an overall measurement of the temperature rise. Measuring the individual pulses in some way (e.g. via de acoustic wave or some other technique that allows high frequency sampling) would probably require reducing the pulse frequency to at least 20 kHz which could maybe be achieved at extraction or alternatively using a rotating stopper). Figures 5e-f show, however, that at 20 kHz an underlying drift starts to form due to the heat diffusion away from the irradiated volume. This could add uncertainty to the individual pulse measurement. On the other hand, after a few tens of ms, a steady state regime is reached in which more accurate measurements may be possible.

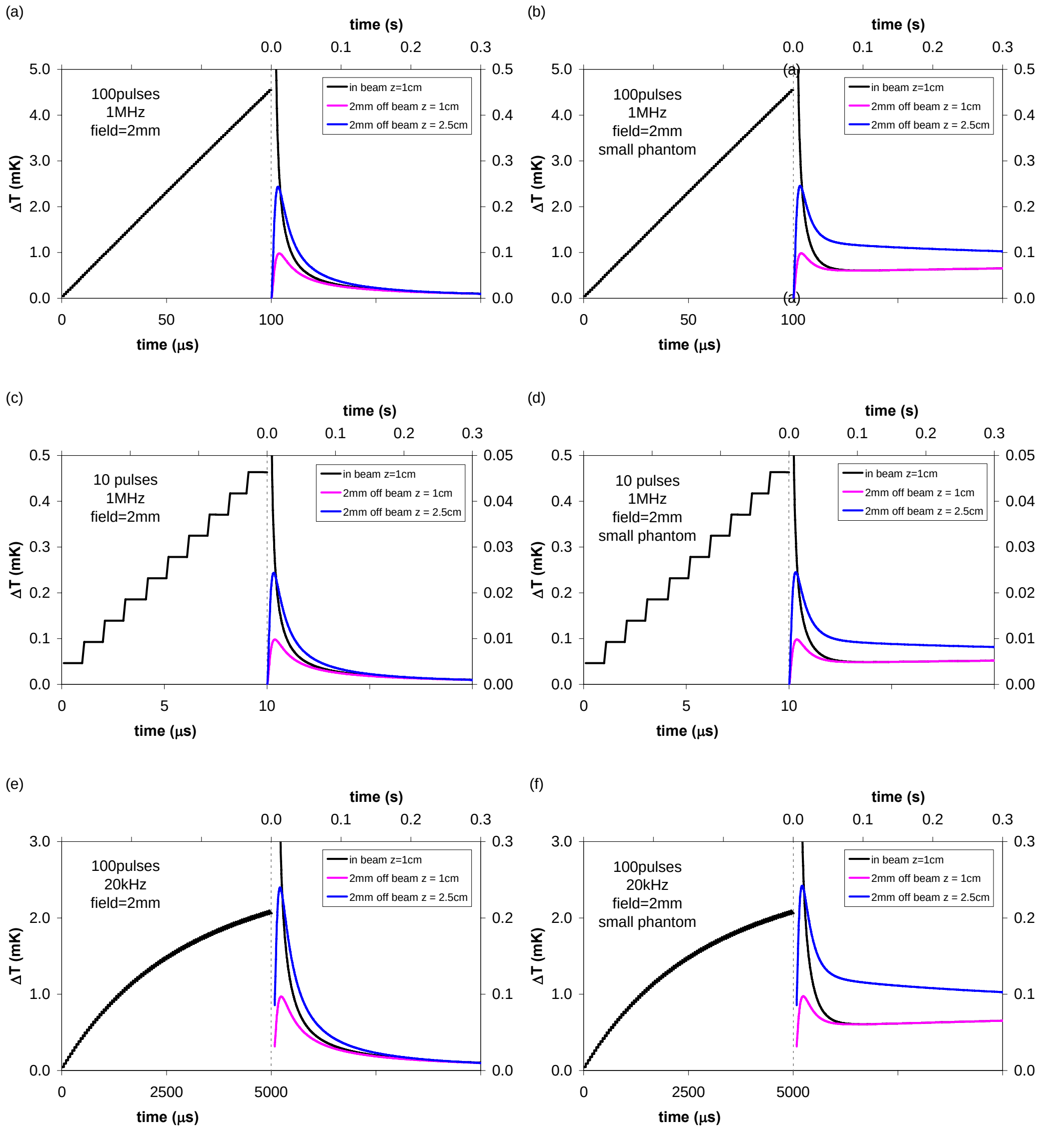

Figure 5. Simulated temperature rise in various points in graphite absorbers of 10 cm diameter and 10 cm length (a, c and d) and 1 cm diameter and 3 cm length (a, c and d) due to the pulse trains of protons. The number of pulses and frequency are given in the graphs. The left pane (left and bottom axis) of each graph shows the temperature rise at 1 cm depth in the beam during the irradiation interval, the right pane (right and top axis) shows at a longer time scale the temperature drifts at three points after the irradiation.

In all the figures it is visible that the drifts after the irradiation interval settle within a few seconds, which could easily be measured with thermistors. Obviously, the final temperature that is reached depends on the phantom size and in this respect it would be preferable for the sake of sensitivity to make the phantom as small as is possible whilst still assuring total absorption of the primary beam and all charged secondary particles.

The figures for aluminium and copper are not shown but they are almost identical, the main difference being that the time constants of the post-irradiation curves, especially for copper, are substantially smaller due to the higher thermal conductivities.

4. CONCLUSIONS

A brief literature review of total absorption calorimeters for proton beams is given. Some features of two calorimeters by Schulz et al. (1990) and Brede et al. (2006) are identified that could be combined in a total absorption calorimeter for dosimetry at the new future 72 MeV proton beam on the SMU site.

Monte Carlo simulations with three different codes show that the energy loss from a graphite, aluminium or copper absorber by neutrons and photons (and internal rest mass conversions) would be around 2%, which should be included as a correction if one wants to measure the energy of the incident proton. The three codes are in reasonable agreement except for a few data points with standard deviations of around 0.2% to 0.3%. An possible experiment at the SMU site, combining a total absorption experiment with a time of flight measurement as an alternative technique to determine the energy of the protons could possibly be used to test which nuclear interaction models are better.

Heat conduction simulations were performed to understand the redistribution of heat in the absorber after irradiation. Given the stability of the temperature distributions in the very short time scale of the pulse trains, pulse per pulse measurement would be possible if very high temperature sampling in the order of 10 MHz would be achievable. With our present day experience of thermistor-based measurements this is not possible given the time constants of the measurement device but alternative techniques could be used for measuring the pulse per pulse absorption, e.g. infrared detection at the absorber front surface or measurement of the acoustic pulses associated with the proton pulses. Both these techniques should at least be achievable at lower pulse rates, such as 20 kHz requiring sample frequencies of the order of 50 kHz, but obviously their sensitivity should be investigated in more detail. The disadvantage of lowering the pulse frequency, however, is that there will be underlying drifts, which may be more difficult to deal with. Going to some steady state regime could reduce this problem.

The total energy deposited by a train of pulses can be measured with thermistors since the equilibrium temperature distribution is established a few seconds after the irradiation. This is long enough for thermistor settling and short enough to avoid substantial energy loss from the absorber to the environment the time constant of which can be increased to hundreds of seconds (by operating in vacuum and further by applying reflective surfaces in order to minimize radiative heat transfer).

Overall, both from the Monte Carlo results as from the heat conduction simulations there appears to be no clear advantage in using either graphite, aluminium or copper as an absorber apart from a slight advantage of copper regarding the time constant of redistributing heat. The choice of the absorber material could thus be dependent on other considerations (e.g. if one wants to measure the acoustic shock wave it may be better to use copper). A combined absorber of the three materials may also be constructed which would enable a comparison of the non-elastic nuclear interaction cross sections for the three materials as well as the heat defect.

5. ACKNOWLEDGEMENTS

This work was funded as part of the UK National Measurement System, Ionising Radiation Metrology Programme and the UK National Measurement Secondment Scheme by the National Measurement System Policy Unit of the UK Department for Innovation, Universities and Skills.

6. REFERENCES

AGOSTINELLI, S. et al. Geant4-A simulation toolkit. *Nucl. Instrum. Methods Phys. Res. A*, 506, 250-303, 2003.

ALLISY-ROBERTS, P.J. and BURNS, D.T. Summary of the BIPM.RI(I)-K4 comparison for absorbed dose to water in ^{60}Co gamma radiation. *Metrologia*, **42**, 06002, 2005.

BERGER, M.J. Proton Monte Carlo transport program PTRAN *National Institute for Standards and Technology Report NISTIR 5113*, NIST, Gaithersburg, USA ,1993.

BREDE, H.J., HECKER, O. and HOLLNAGEL, R. Measurement of the heat defect in water and A-150 plastic for high-energy protons, deuterons, and a particles. *Radiat. Prot. Dosim.*, **70**, 505-8, 1997.

BREDE, H.J., HECKER, O. and HOLLNAGEL, R. An absorbed dose to water calorimeter for collimated radiation fields. *Nucl. Instrum. Meth. A*, **455**, 721-32, 2000.

BREDE, H.J., GREIF, K-D., HECKER, O., HEEG, P., HEESE, J., JONES, D.T.L., KLUGE, H. and SCHARDT, D. Absorbed dose to water determination with ionization chamber dosimetry and calorimetry in restricted neutron, photon, proton and heavy-ion radiation fields. *Phys. Med. Biol.*, **51**, 3667-82, 2006.

FLEMING, D.M. and GLASS W.A. Endothermic Processes in Tissue-Equivalent Plastic. *Radiat. Res.*, **37**, 16-322, 1969.

KAYE, G.W.C and LABY, T.H. Tables of physical and chemical constants, 16th edition, Longman, London, UK, 1995.

LEBLANC, E., DE MARCILLAC, P., CORON, N., LEBLANC, J., LOIDL, M., METGE, J.F. and BOUCHARD, J. A new absolute method for the standardization of radionuclides emitting low-energy radiation. *Appl. Radiat. Isot.*, **56**, 245-51, 2002.

LEBLANC, E., CORON, N., LEBLANC, J., DE MARCILLAC, P., BOUCHARD, J. and PLAGNARD, J. High-energy resolution alpha spectrometry using cryogenic detectors. *Appl. Radiat. Isot.*, **64**, 1281-6, 2006.

MCDONALD, J.C. and GOODMAN, L.J. Measurements of the thermal defect for A-150 plastic. *Phys. Med. Biol.*, **27**, 229-33, 1982.

PAGANETTI, H. and GOTTSCHALK, B. Test of Geant3 and Geant4 nuclear models for 160 MeV protons stopping in CH_2. *Med. Phys.*, **30**, 1926-31, 2003.

PALMANS, H. Experimental verification of simulated excess heat effects in the sealed water calorimeter. *NPL report CIRM 42*, Proceedings of the NPL Calorimetry Workshop, Richmond, UK, 8-10 December 1999, pp. 74-84, 1999.

PALMANS, H. McPTRAN.CAVITY and McPTRAN.RZ, Monte Carlo codes for the simulation of proton beams and calculation of proton detector perturbation factors. *In: The Monte Carlo Method: Versatility Unbounded in a Dynamic Computing World* (Illinois, USA: American Nuclear Society), 2005

PALMANS, H. and VERHAEGEN, F. Calculated depth dose distributions for proton beams in some low-Z materials. *Phys. Med. Biol.*, **42**, 1175-83, 1997.

PALMANS, H., THOMAS, R., SIMON, M., DUANE, S., KACPEREK, A., DUSAUTOY, A. and VERHAEGEN, F. A small-body portable graphite calorimeter for dosimetry in low-energy clinical proton beams. *Phys. Med. Biol.*, 49, 3737-49, 2004.

PALMANS, H., THOMAS, R., SHIPLEY, D. and KACPEREK, A. Light-ion beam dosimetry. *NPL report DQL-RD 003*, 2006

SCHULZ, R.J., VENKATARAMANAN, N. and HUQ, M.S. The thermal defect of A-150 plastic and graphite for low-energy protons. *Phys. Med. Biol.*, **35**, 1563-74, 1990.

SELBACH, H-J., HOHLFELD, K. and KRAMER, H.M. An Experimental Method for Measuring the Heat Defect of Water Using Total Absorption of Soft X-Rays. *Metrologia*, **29**, 341-7, 1992.

STUMP, K.E., DEWERD, L.A., RUDMAN, D.A. and SCHIMA, S.A. Active radiometric calorimeter for absolute calibration of radioactive sources. *Rev. Sci. Instrum.*, **76**, 033504, 2005.

TWERENBOLD, D. Cryogenic particle detectors. *Rep. Prog. Phys.*, **59**, 349–426, 1996.

WATERS, L.S. MCNPX-User's Manual Version 2.4.0. Los Alamos National Laboratory, Los Alamos, NM, USA, 2002.